

# Cobalamin-Dependent Methionine Synthase: Probing the Role of the Axial Base in Catalysis of Methyl Transfer between Methyltetrahydrofolate and Exogenous Cob(I)alamin or Cob(I)inamide<sup>†</sup>

Jeanne Sirovatka Dorweiler,<sup>‡,§</sup> Richard G. Finke,<sup>||</sup> and Rowena G. Matthews<sup>\*,‡</sup>

Biophysics Research Division, Life Sciences Institute, and Department of Biological Chemistry, University of Michigan, Ann Arbor, Michigan 48109, and Chemistry Department, Colorado State University, Ft. Collins, Colorado 80523

Received August 26, 2003; Revised Manuscript Received October 9, 2003

**ABSTRACT:** Cobalamin-dependent methionine synthase (MetH) catalyzes the transfer of methyl groups between methyltetrahydrofolate (CH<sub>3</sub>-H<sub>4</sub>folate) and homocysteine, with the enzyme-bound cobalamin serving as an intermediary in the methyl transfers. An MetH fragment comprising residues 2–649 contains modules that bind and activate CH<sub>3</sub>-H<sub>4</sub>folate and homocysteine and catalyze methyl transfers to and from exogenous cobalamin. Comparison of the rates of reaction of cobalamin, which contains a dimethylbenzimidazole nucleotide coordinated to the cobalt in the lower axial position, and cobinamide, which lacks the dimethylbenzimidazole nucleotide, allows assessment of the degree of stabilization the dimethylbenzimidazole base provides for methyl transfer between CH<sub>3</sub>-H<sub>4</sub>folate bound to MetH(2–649) and exogenous cob(I)alamin. When the reactions of cob(I)alamin or cob(I)inamide with CH<sub>3</sub>-H<sub>4</sub>folate are compared, the observed second-order rate constants are 2.7-fold faster for cob(I)alamin; in the reverse direction, methylcobinamide reacts 35-fold faster than methylcobalamin with enzyme-bound tetrahydrofolate. These measurements can be used to estimate the influence of the dimethylbenzimidazole ligand on both the thermodynamics and kinetics of methyl transfer between methyltetrahydrofolate and cob(I)alamin or cob(I)inamide. The free energy change for methyl transfer from CH<sub>3</sub>-H<sub>4</sub>folate to cob(I)alamin is 2.8 kcal more favorable than that for methyl transfer to cob(I)inamide. Dimethylbenzimidazole contributes ~0.6 kcal/mol of stabilization for the forward reaction and ~2.2 kcal/mol of destabilization for the reverse reaction. Binding of methylcobalamin to full-length methionine synthase is accompanied by ligand substitution, and switching between “base-on” and “base-off” states of the cofactor has been demonstrated [Bandarian, V., et al. (2003) *Proc. Natl. Acad. Sci. U.S.A.* 100, 8156–8163]. The present results disfavor a major role for such switching in catalysis of methyl transfer, and are consistent with the hypothesis that the primary role of the ligand triad in methionine synthase is controlling the distribution of enzyme conformations during catalysis.

Cobalamin-dependent methionine synthase (MetH<sup>1</sup>) catalyzes the terminal step in the de novo biosynthesis of methionine in *Escherichia coli*. As shown in Figure 1, the cobalamin prosthetic group serves as an intermediary in the reaction. Methionine is generated by a methyl transfer to homocysteine from methylcobalamin (structure shown in Figure 2), yielding methionine and cob(I)alamin. To regenerate methylcobalamin, a methyl group is transferred from

CH<sub>3</sub>-H<sub>4</sub>folate to cob(I)alamin, forming methylcobalamin and H<sub>4</sub>folate. Methionine synthase is a modular enzyme (7–9); the enzyme binds each substrate and the metallocofactor in distinct regions, as shown in Figure 3. The first two modules bind CH<sub>3</sub>-H<sub>4</sub>folate and homocysteine, the third module binds methylcobalamin, and the fourth module binds AdoMet and is responsible for reductive methylation of enzyme in the cob(II)alamin form. This C-terminal module contains determinants for the binding of flavodoxin, the electron donor to cob(II)alamin during reductive activation (10).

The chemical mechanism that has been commonly proposed for the methyl transfer reaction is a proton-assisted S<sub>N</sub>2 mechanism, shown in Figure 4. Stereochemical studies (11) of the overall methyl transfer from CH<sub>3</sub>-H<sub>4</sub>folate to homocysteine demonstrated retention in configuration of the transferred methyl group, consistent with two successive methyl transfers each occurring with inversion, e.g., two S<sub>N</sub>2 transfers. Chemical precedent studies for this mechanism demonstrate that quaternary amines will react with cobalamin analogues such as cob(I)aloxime (14). Cob(I)alamin also reacted in these studies, but only in low, unquantified, yield.

<sup>†</sup> This work has been supported in part by NIH Grant GM24908 (R.G.M.) and by NIH Postdoctoral Fellowship HD10173 (J.S.D.).

\* To whom correspondence should be addressed. E-mail: rmatthew@umich.edu.

<sup>‡</sup> University of Michigan.

<sup>§</sup> Present address: 2nd Brigade, 91st Division, U.S. Army, Ft. Carson, CO 80913.

<sup>||</sup> Colorado State University.

<sup>1</sup> Abbreviations: MetH, cobalamin-dependent methionine synthase; CH<sub>3</sub>-H<sub>4</sub>folate, 5-methyltetrahydrofolate; H<sub>4</sub>folate, tetrahydrofolate; Hcy, l-homocysteine; MeCbl, methylcobalamin; MeCbi<sup>+</sup>, methylcobinamide; Co(I)Cbl<sup>+</sup>, cob(I)alamin; Co(I)Cbi, cob(I)inamide; Co(II)Cbl, cob(II)alamin; Co(II)Cbi<sup>+</sup>, cob(II)inamide; py, pyridine; bzm, 5,6-dimethylbenzimidazole; PhNMe<sub>3</sub><sup>+</sup>, trimethylanilinium (phenyltrimethylammonium) cation.

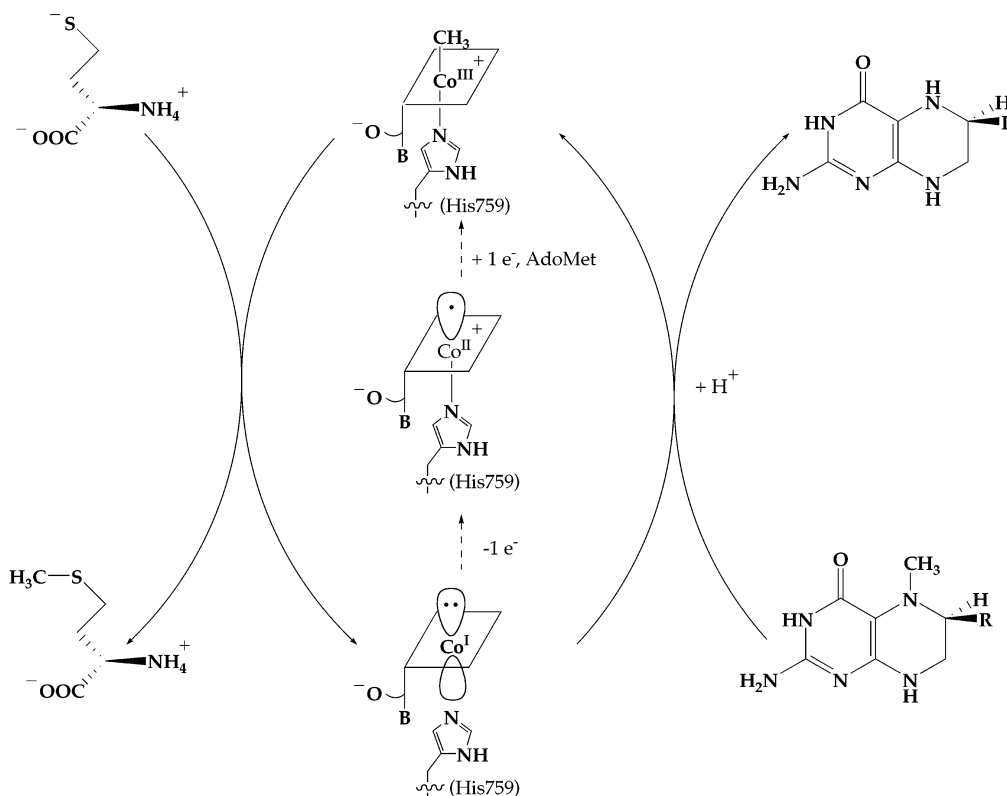


FIGURE 1: A schematic representation of the catalytic cycle of methionine synthase. The substrates homocysteine and methyltetrahydrofolate are bound to separate sites within the holoenzyme. Homocysteine is deprotonated upon binding to the enzyme (6) and is, therefore, represented here as a thiolate anion. During catalytic turnover, the cobalamin cofactor cycles between base-off histidine-on methylcob(III)alamin and base-off cob(I)alamin. In the first half-reaction, methylcobalamin formally transfers a methyl cation to the homocysteine thiolate, generating methionine and cob(I)alamin. In the second half-reaction, the methyl cation is transferred from methyltetrahydrofolate to cob(I)alamin, generating methylcobalamin and tetrahydrofolate. Periodically, cob(I)alamin is oxidized to inactive cob(II)alamin, which is then converted to methylcobalamin by a reductive methylation involving electron transfer from reduced flavodoxin and methyl group donation from *S*-adenosylmethionine.

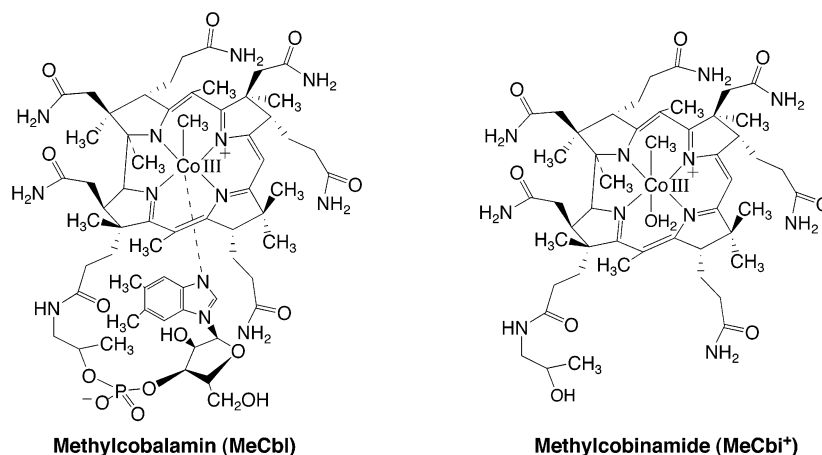


FIGURE 2: Structures of methylcobalamin and methylcobinamide.

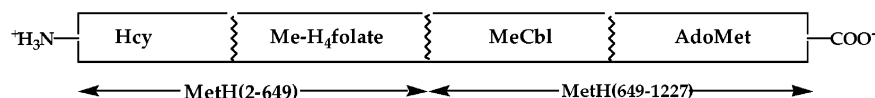


FIGURE 3: Modular domains of methionine synthase. MetH(2–649), the enzymatic fragment used in this work, is a 71 kDa fragment of MetH containing the modules that bind Hcy and CH<sub>3</sub>-H<sub>4</sub>folate (8).

Methyl transfer from dimethylaniline to a cob(I)yrinate model has recently been demonstrated under acidic conditions, where the amine would be protonated (15), or by using Zn<sup>2+</sup> as a Lewis acid (16). The only kinetic measurement of a methyl transfer involving cobalamin is the reaction of the quaternized trimethylphenylammonium cation, PhNMe<sub>3</sub><sup>+</sup>,

with cob(I)alamin, which is characterized by a second-order rate constant of  $k_2 = 2 \times 10^{-3} \text{ M}^{-1} \text{ s}^{-1}$  (17). All of these model studies are consistent with S<sub>N</sub>2 mechanisms in which the amine leaving group is activated by protonation at nitrogen, by quaternization, or by coordination to a Lewis acid.

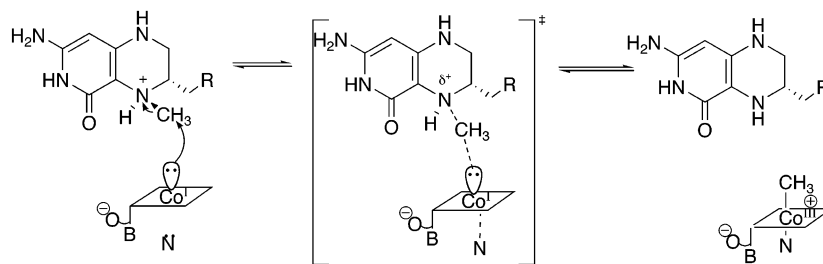


FIGURE 4: A proton-assisted  $S_N2$  mechanism for methionine synthase. We have shown methyltetrahydrofolate as protonated prior to group transfer since the unprotonated form is an ineffective leaving group, and since studies herein and elsewhere (12) are consistent with this hypothesis, but the exact timing of proton vs group transfer is not definitively known. The stereochemistry at N5 is drawn on the basis of an X-ray structure of the Hcy-binding and folate-binding domains of MetH from *Thermatoga maritima* with  $\text{CH}_3\text{-H}_4\text{folate}$  bound that was recently determined in the laboratory of Martha Ludwig (13).

The group transfer from  $\text{CH}_3\text{-H}_4\text{folate}$  to cob(I)alamin shown in Figure 4 would be expected to be accompanied by changes in the bonding of the dimethylbenzimidazole base as the reaction progresses. Cob(I)alamin prefers to be four-coordinate, while methylcobalamin shows strong coordination of its nitrogeneous axial dimethylbenzimidazole ligand.<sup>2</sup> If a bond between cobalt and the nitrogeneous axial ligand develops in the transition state, then the prediction is that the transition state will be stabilized in the presence of a dimethylbenzimidazole ligand. If, however, cobalamin is replaced by cobinamide, with its relatively weak axial ligation to a solvent molecule, then there can be no  $\text{Co-N}$  bond formation and thus little resultant stabilization of the transition state by the lower axial ligand. The predicted net result will be a lower  $\Delta G_r^\ddagger$  value for the reaction of cob(I)alamin as compared to that for cob(I)inamide.

When the reaction is measured in the reverse direction, namely, attack of  $\text{H}_4\text{folate}$  on methylcobalamin, bonding to dimethylbenzimidazole is predicted to stabilize the ground state of methylcobalamin more than the transition state, which is moving toward the base-off cob(I)alamin form. If methylcobalamin is replaced by methylcobinamide, the weaker axial ligation in the ground state is predicted to result in less ground-state stabilization. The predicted net result will be a higher  $\Delta G_r^\ddagger$  value for the methylcobalamin reaction compared to that for methylcobinamide. If all bonding to the axial ligand were lost in the transition state, the decrease in the rate of reaction of methylcobalamin as compared to methylcobinamide should be directly related to the  $\Delta\Delta G_{\text{rxn}}$ . Any bonding in the transition state will lead to a diminished slowing of the reaction of methylcobalamin as compared to methylcobinamide. In summary, comparing the rates of reaction of folate substrates bound to MetH with exogenous cobalamin or cobinamide allows us to probe the involvement of the axial base in the transition state for the reaction. Is stabilization by the axial base critical for methyl transfer?

Reaction of full-length MetH with its folate substrates involves methyl transfers to and from the bound cobalamin cofactor, and does not require added cobalamin because the cofactor is tightly bound and does not dissociate. Although the full-length enzyme retains the ability to catalyze methyl transfers between bound folate substrates and exogenous cobalamin (8), the absorbance of the bound cofactor com-

plicates measurements of these reactions using UV-vis absorbance spectroscopy. Therefore, we have found it convenient to employ a fragment of the enzyme, MetH(2-649), which lacks the cobalamin-binding module of the full-length protein but retains the ability to bind both  $\text{CH}_3\text{-H}_4\text{folate}$  and  $\text{H}_4\text{folate}$ , and to catalyze methyl transfers between these substrates and exogenous cob(I)alamin and methylcobalamin (8). These reactions are first-order in exogenous cobalamin and in enzyme concentration, and the second-order rate constants can be compared with those for model chemical reactions.

## MATERIALS AND METHODS

**Materials.**  $\text{MeCbi}^+\text{BF}_4^-$  was synthesized as previously described (3), and stored in the dark at 0 °C.  $\text{K}_2\text{HPO}_4\cdot 3\text{H}_2\text{O}$ ,  $\text{KH}_2\text{PO}_4$ , guanidine, 4-(hydroxymercurio)benzoic acid, sodium salt, 5,5'-dithiobis(2-nitrobenzoic acid) (Ellman's reagent), and 4-(2-pyridylazo)resorcinol (PAR) were obtained from Sigma and stored at room temperature. Titanium(III) chloride, a 30% w/v solution in 2 N HCl, was obtained from Acros and stored at room temperature. Pyridine (99.8%, anhydrous) was obtained from Aldrich and stored at room temperature. Trimethylphenylammonium chloride and iodide were obtained from Aldrich and recrystallized from hot acetonitrile before use. (6S)-Tetrahydrofolic acid, sodium salt, and (6S)-methyltetrahydrofolic acid, sodium salt, were generous gifts from Eprova, and were stored at 0 °C. All water was purified by Barnstead NANOpure filtration prior to use, to yield a resistivity of  $\geq 18 \text{ M}\Omega/\text{cm}$ .

**Instrumentation.** UV-vis spectra were obtained on an HP 8452A diode array spectrophotometer attached to an HP Vectra computer, and equipped with an HP89090A peltier temperature controller set to maintain the internal cell temperature at  $37 \pm 0.1$  °C.

**MetH(2-649).** The 71 kDa N-terminal fragment of methionine synthase was overexpressed and purified to apparent homogeneity as previously described (8). Enzyme purity was determined to be  $>95\%$  by SDS-PAGE. Enzyme concentration was determined by measuring the zinc content as described previously (18), except that 4-(hydroxymercurio)benzoic acid, sodium salt, was used instead of *p*-(hydroxymercurio)phenylsulfonic acid in the zinc assay, since the latter compound is no longer commercially available. Use of 4-(hydroxymercurio)benzoic acid gives the same final zinc concentration as the earlier compound within experimental error, as determined by control experiments using both reagents on samples from the same enzyme preparation.

<sup>2</sup> The preferred coordination states for methylcobalamin and cob(I)alamin have been extensively discussed in the literature (1). Occupancy of the  $d_{z^2}$  orbital in cob(I)alamin leads to a  $\text{Co-N}(\text{bzm})$   $\sigma$ -antibonding interaction which disfavors coordination of the base (2).

**Titanium(III) Citrate Preparation.** Titanium(III) citrate was prepared as described in the literature (19) by degassing 2 mL of  $\text{TiCl}_3$  (in 2 N HCl) by repeated cycling between argon and a vacuum, followed by addition of 18 mL of degassed 0.5 M sodium citrate using an airtight syringe. The resulting solution was stirred at room temperature under argon for 30 min; 6 mL of degassed, saturated  $\text{NaHCO}_3$  solution and 14 mL of degassed, 1 M Tris base solution were then added to the original solution using an airtight syringe. The resulting solution was stirred at room temperature overnight under argon. The titanium(III) citrate solution was stored at room temperature under argon and protected from light; lightening of the dark brown color during storage indicates degradation, at which point the titanium(III) citrate was discarded.

**Spectrophotometric  $\text{CH}_3\text{-H}_4\text{folate:Cob(I)alamin Methyl Transfer Assay.}$**  This assay was performed as described previously (8). The  $\text{CH}_3\text{-H}_4\text{folate}$  solution was prepared in air by dissolving the solid in 50 mM potassium phosphate buffer, pH 7.2, to give a 20 mM stock solution. In a 0.4 cm path length anaerobic cuvette equipped with a side arm, hydroxocobalamin and MetH(2–649) at the indicated concentrations were combined. The  $\text{CH}_3\text{-H}_4\text{folate}$  solution was loaded into the side arm. The solution was made anaerobic by 4 series of 10 cycles of exposure to a vacuum, followed by replacement with argon, over a period of 20 min. After degassing, 100  $\mu\text{L}$  of the titanium(III) citrate solution was added to the cuvette with an airtight syringe through a septum. The solution changed color from pink to brown-black, indicating the formation of cob(I)alamin. The cuvette was warmed at 37 °C in the cell holder for 10 min, and the reaction initiated by tipping the  $\text{CH}_3\text{-H}_4\text{folate}$  solution into the cuvette. The reaction was followed at 520 nm, the  $\lambda_{\text{max}}$  for methylcobalamin using the differential extinction coefficient (methylcobalamin – cob(I)alamin) of  $6045 \text{ M}^{-1} \text{ cm}^{-1}$ . The initial rate of methylcobalamin formation and its associated standard error were determined by graphing the raw absorbance data, fitting a line to the initial points (typically 4–5), and then importing the data points used for the fit into Excel. The linear least-squares tool in Excel was used to determine the errors associated with that rate measurement. The initial rate of methylcobalamin formation was converted to a second-order rate constant by dividing by the initial concentrations of HOCbl and enzyme.

**Spectrophotometric  $\text{CH}_3\text{-H}_4\text{folate:Cob(I)inamide Methyl Transfer Assay.}$**  This assay was similar to the cobalamin assay described above, except that the starting solution (containing methylcobinamide and MetH(2–649) in the main cuvette and  $\text{CH}_3\text{-H}_4\text{folate}$  in the side arm) was exposed to laboratory light while being degassed, photolyzing methylcobinamide to cob(II)inamide. Once cob(II)inamide was completely formed (as followed by the increase in absorbance at 468 nm, the  $\lambda_{\text{max}}$  for cob(II)inamide), 60  $\mu\text{L}$  of degassed titanium(III) citrate solution was added using an airtight syringe to generate cob(I)inamide. After  $\text{CH}_3\text{-H}_4\text{folate}$  was tipped in, the reaction was followed at 462 nm, the  $\lambda_{\text{max}}$  for methylcobinamide, using a differential extinction coefficient (methylcobinamide – cob(I)inamide) of  $7740 \text{ M}^{-1} \text{ cm}^{-1}$ . The initial rate of methylcobinamide formation was converted to a second-order rate constant by dividing by the initial concentrations of cob(II)inamide and enzyme. Determination of the standard errors was performed as described for the  $\text{CH}_3\text{-H}_4\text{folate:cob(I)alamin methyl transferase assay.}$

**Spectrophotometric  $\text{Methylcobalamin:H}_4\text{folate Methyl Transfer Assay.}$**  This assay was performed as described previously (8). A  $\text{H}_4\text{folate}$  stock solution (40 mM) was prepared by dissolving the solid  $\text{H}_4\text{folate}$  in degassed 50 mM potassium phosphate buffer, pH 7.2, under argon in a Schlenk tube (a vessel equipped with a side arm and a stopcock for anaerobic work (20)). The assay was carried out in a darkened room under anaerobic conditions using a quartz 0.4 cm path length Schlenk cuvette equipped with a side arm. The initial reaction mixture, placed in the cell of the Schlenk cuvette, contained methylcobalamin and MetH(2–649) at the indicated concentrations in 50 mM potassium phosphate buffer, pH 7.2, and the cuvette was degassed by repeated evacuation/equilibration with argon over 20 min. The degassed  $\text{H}_4\text{folate}$  solution was then transferred using an airtight syringe from the Schlenk tube through a septum into the side arm of the Schlenk cuvette. The cuvette was warmed at 37 °C in the cell holder for 5 min before the reaction was started by tipping the  $\text{H}_4\text{folate}$  solution from the side arm into the main cuvette. The reaction was monitored at 538 nm, the isosbestic point between cob(I)alamin and cob(II)alamin, to make the analysis insensitive to oxidation of cob(I)alamin to cob(II)alamin. A differential extinction coefficient of  $4540 \text{ M}^{-1} \text{ cm}^{-1}$  at 538 nm (methylcobalamin – cob(I/II)alamin) was used to convert the change in absorbance to moles of methylcobalamin formed per second. The initial rate of disappearance of methylcobalamin was converted to a second-order rate constant by dividing by the initial concentrations of methylcobalamin and MetH(2–649). Determination of the standard errors was performed as described for the  $\text{CH}_3\text{-H}_4\text{folate:cob(I)alamin methyl transferase assay.}$

**Spectrophotometric  $\text{Methylcobinamide:H}_4\text{folate Methyl Transfer Assay.}$**  This assay was similar to the methylcobalamin: $\text{H}_4\text{folate}$  assay described above. Initial rates, associated errors, and second-order rate constants were derived as described above, using a differential extinction coefficient at 462 nm (methylcobinamide – cob(I)inamide) of  $7740 \text{ M}^{-1} \text{ cm}^{-1}$ .

**Addition of Pyridine to the  $\text{Methylcobalamin:H}_4\text{folate}$ ,  $\text{CH}_3\text{-H}_4\text{folate:Cob(I)alamin}$ ,  $\text{Methylcobinamide:H}_4\text{folate}$ , and  $\text{CH}_3\text{-H}_4\text{folate:Cob(I)inamide Methyl Transfer Assays.}$**  To test the effects of added exogenous bases on enzyme stability in the methyl transfer assays, aliquots of neat pyridine (62, 124, 185, 247, and 309 mM final concentrations) were added to solutions of MetH(2–649) and cobalamin or cobinamide at the indicated concentrations. The initial rates were measured as described for the corresponding assays in the absence of pyridine and converted into second-order rate constants.

**Kinetic Studies on Reactions of Cob(I)alamin and Cob(I)inamide with  $\text{PhNMe}_3^+$  Salts.** In a 0.4 cm path length Schlenk cuvette, a solution of cob(I)alamin in 50 mM potassium phosphate buffer, pH 7.2, was prepared by photolyzing methylcobalamin and then reducing the resultant cob(II)alamin with titanium(III) citrate. Portions of a 2.5 M stock solution of  $\text{PhNMe}_3^+\text{Cl}^-$  in 50 mM  $\text{KP}_i$  buffer, pH 7.2, were placed in the side arm, and the solutions were degassed. The reaction was initiated at 25 °C by tipping the  $\text{PhNMe}_3^+\text{Cl}^-$  solution into the main cuvette. The reaction was followed by UV–vis spectroscopy at 386 nm, the  $\lambda_{\text{max}}$  for cob(I)alamin, and 520 nm, the  $\lambda_{\text{max}}$  for methylcobalamin. Similar experiments were conducted using  $\text{PhNMe}_3^+\text{I}^-$  to



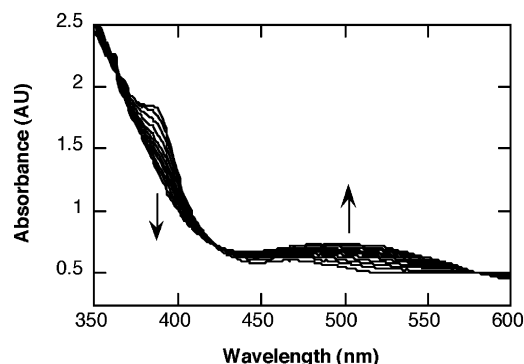


FIGURE 5: Absorbance changes associated with the conversion of cob(I)alamin to methylcobalamin upon the addition of  $\text{CH}_3\text{-H}_4\text{folate}$  in the presence of MetH(2–649). The initial concentrations of the components after mixing were  $\text{CH}_3\text{-H}_4\text{folate}$ , 1 mM; MetH(2–649), 3.3  $\mu\text{M}$ ; and hydroxocobalamin, 180  $\mu\text{M}$ . The cob(I)alamin spectrum below 400 nm is partially obscured by the absorbance of excess titanium citrate, the added reducing agent. The experiment was conducted in a 0.4 cm path length cell.

test the effect of changing the counteranion, except that the highest final concentration of  $\text{PhNMe}_3^+\text{I}^-$  employed was 0.5 M, rather than 1 M, due to the lower solubility of the iodide salt in 50 mM phosphate buffer.

## RESULTS

**Methyl Transfer from  $\text{CH}_3\text{-H}_4\text{folate}$  to Cob(I)alamin Catalyzed by MetH(2–649).** We followed the methylation of cob(I)alamin with (6*S*)- $\text{CH}_3\text{-H}_4\text{folate}$  catalyzed by MetH(2–649) by UV–vis absorbance spectroscopy, observing the increase in absorbance at 520 nm associated with methylcobalamin formation (Figure 5). The final concentration of methylcobalamin, as assessed using an extinction coefficient of 9100  $\text{M}^{-1}\text{cm}^{-1}$  at 520 nm (21), indicated 100%  $\pm$  10% conversion of the initial hydroxocobalamin to product. The overall reaction is first-order in both cob(I)alamin and MetH(2–649), as previously reported (8). Previous studies of April Smith have shown that the reaction exhibits a saturable dependence on  $\text{CH}_3\text{-H}_4\text{folate}$ , with an apparent  $K_m$  of 60  $\mu\text{M}$  (12), so the experiment shown in Figure 5 was conducted in the presence of a saturating concentration of  $\text{CH}_3\text{-H}_4\text{folate}$ . The calculated second-order rate constant for this reaction at 37  $^\circ\text{C}$ , averaged from five independent experiments, is  $620 \pm 40\text{ M}^{-1}\text{s}^{-1}$ , in good agreement with the published value of  $590\text{ M}^{-1}\text{s}^{-1}$  (8).

**Methyl Transfer from  $\text{CH}_3\text{-H}_4\text{folate}$  to Cob(I)inamide Catalyzed by MetH(2–649).** The rate of reaction of cob(I)inamide with (6*S*)- $\text{CH}_3\text{-H}_4\text{folate}$  catalyzed by MetH(2–649) was monitored by UV–vis absorbance spectroscopy, observing the increase in absorbance associated with methylcobinamide formation at 462 nm (Figure 6). In these experiments, methylcobinamide was initially added to the cuvette, and cob(II)inamide was generated by photolysis during degassing. The cob(II)inamide was reduced to cob(I)inamide on addition of titanium citrate. The final concentration of methylcobinamide, as assessed using an extinction coefficient of 11100  $\text{M}^{-1}\text{cm}^{-1}$  at 462 nm (12), indicated 85%  $\pm$  10% conversion of the initially added methylcobinamide to product. Titanium citrate has a broad absorbance peak, complicating assessment of the extent of reaction from the final spectrum. We estimated the initial concentration of methylcobinamide (prior to photolysis and reduction) in our experiments by diluting

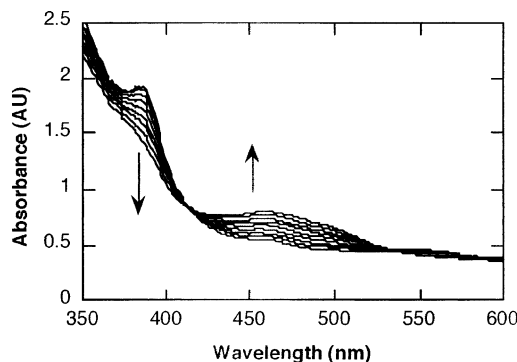


FIGURE 6: Absorbance changes associated with the conversion of cob(I)inamide to methylcobinamide on the addition of  $\text{CH}_3\text{-H}_4\text{folate}$  in the presence of MetH(2–649). Before initiation of the reaction, methylcobinamide was converted to cob(II)inamide by photolysis and reduction with titanium(III) citrate. The initial concentrations of the components after mixing were  $\text{CH}_3\text{-H}_4\text{folate}$ , 1 mM; MetH(2–649), 3.3  $\mu\text{M}$ ; and methylcobinamide, 150  $\mu\text{M}$ . The cob(I)inamide spectrum below 400 nm is partially obscured by the absorbance of excess titanium citrate, the added reducing agent. The experiment was conducted in a 0.4 cm path length cell.

an identical aliquot of methylcobinamide into buffer lacking titanium citrate and measuring the absorbance. However, the extent of reaction could only be determined from the change in absorbance at 462 nm, and because the reaction requires only  $\sim 100$  s, the yield will be decreased by any reaction that has occurred between mixing and the initiation of data collection. While experiments with cob(I)alamin and  $\text{CH}_3\text{-H}_4\text{folate}$  also are conducted in the presence of titanium citrate, the reactions are slower, and the estimated yield is approximately stoichiometric.

The reaction was shown to be first-order in both cobinamide and MetH(2–649) by showing a linear dependence of the initial rate of product formation on [cob(I)inamide] (Figure A, Supporting Information) and [MetH(2–649)] (Figure B, Supporting Information). The rate constants determined from these plots were 183  $\text{M}^{-1}\text{s}^{-1}$  (A) and 220  $\text{M}^{-1}\text{s}^{-1}$  (B). The calculated second-order rate constant for this reaction averaged from five independent experiments conducted under identical conditions is  $230 \pm 10\text{ M}^{-1}\text{s}^{-1}$ , approximately 3-fold less than the rate constant for reaction of cob(I)alamin.

**Methyl Transfer from Methylcobalamin to  $\text{H}_4\text{folate}$  Catalyzed by MetH(2–649).** The reaction was followed by UV–vis spectroscopy, observing the decrease at 520 nm (the  $\lambda_{\text{max}}$  of methylcobalamin), and the increase at 474 nm (the  $\lambda_{\text{max}}$  of cob(II)alamin), as shown in Figure 7. In the presence of  $\text{H}_4\text{folate}$ , cob(I)alamin is initially formed, but rapidly oxidizes (8); the observed reaction is the conversion of methylcobalamin to cob(II)alamin. The second-order rate constant for  $\text{CH}_3\text{-H}_4\text{folate}$  formation was derived from data taken at 538 nm, the isosbestic point between cob(I)alamin and cob(II)alamin. The calculated second-order rate constant, averaged from five independent experiments, is  $81 \pm 10\text{ M}^{-1}\text{s}^{-1}$ , in excellent agreement with the value of  $80 \pm 13\text{ M}^{-1}\text{s}^{-1}$  determined previously (12).

**Methyl Transfer from Free Methylcobinamide to  $\text{H}_4\text{folate}$  Catalyzed by MetH(2–649).** The analogous reaction with methylcobinamide was monitored by observing the decrease in absorbance at 462 nm (the  $\lambda_{\text{max}}$  of methylcobinamide), and the increase at 386 nm (the  $\lambda_{\text{max}}$  of cob(I)inamide), and is shown in Figure 8. In this reaction, the formation of cob(I)-

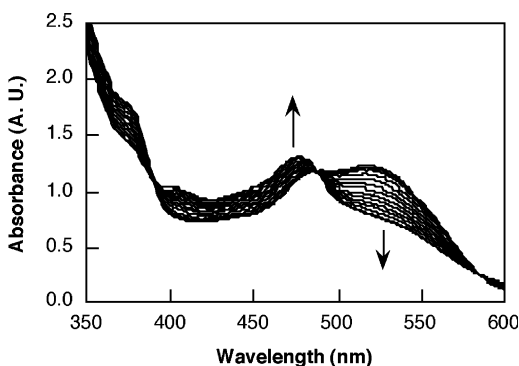


FIGURE 7: Absorbance changes associated with the conversion of methylcobalamin to cob(II)alamin on the addition of  $H_4$ folate in the presence of MetH(2–649). The initial concentrations of the components after mixing were  $H_4$ folate, 3 mM; MetH(2–649), 25  $\mu$ M; and methylcobalamin, 400  $\mu$ M. In experiments previously performed by April Smith, the rate of reaction was shown to exhibit a saturable dependence on  $H_4$ folate, with an apparent  $K_m$  of 400  $\mu$ M at pH 7.2 (12). This experiment was conducted in a 0.4 cm path length cell.

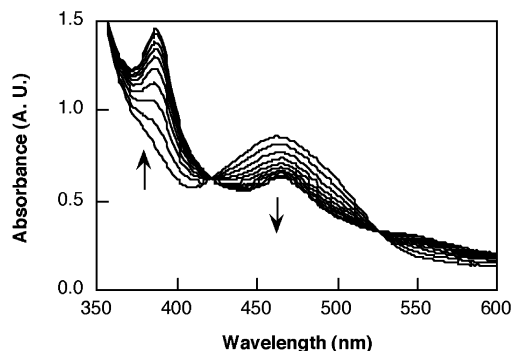


FIGURE 8: Absorbance changes observed for the conversion of methylcobinamide to cob(I)inamide on addition of  $H_4$ folate in the presence of MetH(2–649). The initial concentrations of the components after mixing were  $H_4$ folate, 3 mM; MetH(2–649), 10  $\mu$ M; and methylcobinamide, 200  $\mu$ M. The experiment was conducted in a 0.4 cm path length cell.

inamide is much faster than subsequent oxidation to cob(II)-inamide; hence, a clean conversion is seen from methylcobinamide to cob(I)inamide, with isosbestic points at 421 and 525 nm. Following formation of cob(I)inamide, slow oxidation to cob(II)inamide is observed over about 2000 s. The reaction was shown to be first-order in both methylcobinamide (Figure C, Supporting Information) and MetH(2–649) (Figure D, Supporting Information). The second-order rate constant determined from the data in Figure D is  $3170 \text{ M}^{-1} \text{ s}^{-1}$ . The second-order rate constant averaged from four independent experiments conducted under identical conditions is  $2800 \pm 400 \text{ M}^{-1} \text{ s}^{-1}$ , 35-fold higher than the rate constant for reaction of methylcobalamin. The second-order rate constants for the methyl transfer reactions involving cobinamide and cobalamin are summarized in Table 1.

**Effect of Pyridine on Methyl Transfers to and from Cobalamin and Cobinamide.** Addition of pyridine to the methylcobalamin: $H_4$ folate methyltransferase assay leads to substantial inhibition of activity (Figure E, Supporting Information), despite the fact that pyridine would be expected to compete poorly with the intramolecular dimethylbenzimidazole ligand for occupancy of the lower axial position of methylcobalamin. However, inhibition of enzyme activity is commonly seen in organic solvents (22, 23). When

pyridine was added to the methylcobinamide: $H_4$ folate methyltransferase assay, the observed inhibition at any of the pyridine concentrations examined was greater than that seen in the methylcobalamin: $H_4$ folate methyltransferase assay (Figure E, Supporting Information). These observations suggest an additional inhibitory effect of pyridine in binding to the lower axial position of methylcobinamide and decreasing the rate of reaction. The second-order rate constant for the methylcobinamide: $H_4$ folate methyltransferase assay is  $2800 \text{ M}^{-1} \text{ s}^{-1}$ , while that for the methylcobalamin: $H_4$ folate methyltransferase assay is  $81 \text{ M}^{-1} \text{ s}^{-1}$ , so the effect of pyridine binding to methylcobinamide on the reaction rate is expected to be substantial, even after correction for the inhibition observed in the methylcobalamin: $H_4$ folate methyltransferase assay. Measurements of the binding of pyridine to methylcobinamide under the conditions of the methylcobinamide: $H_4$ folate methyltransferase assay are shown in Figure F (Supporting Information) and yield an association constant of  $6.2 \pm 0.6 \text{ M}^{-1}$ . Figure G (Supporting Information) shows a plot of the corrected second-order rate constant measured for the methylcobinamide: $H_4$ folate methyltransferase assay in the presence of pyridine vs the percent base-on methylcobinamide calculated from the data in Figure F of the Supporting Information. The observed inhibition is roughly proportional to the percent base-on methylcobinamide at that concentration of pyridine.

**Comparison of Solution Rate Constants with Enzymatic Rate Constants for Model Reactions Involving Cob(I)alamin/Cob(I)inamide and  $PhNMe_3^+$ .** While the rates of reaction of methylcobalamin and methylcobinamide with alkanethiolates have been compared (5), model studies comparing the rates of reaction of cob(I)alamin and cob(I)inamide with alkylating agents have not been performed. We compared the rates of reaction of cob(I)alamin and cob(I)inamide with trimethylphenylammonium cation,  $PhNMe_3^+$ . For these studies we used both the chloride and iodide salts of  $PhNMe_3^+$ . We found that cob(I)alamin reacted with  $PhNMe_3^+$  in 50 mM potassium phosphate buffer at 25 °C to generate methylcobalamin and  $PhNMe_2$ . The reaction is first-order in both cob(I)alamin and  $PhNMe_3^+$  (Figure H, Supporting Information), allowing calculation of the second-order rate constants shown in Table 2. Similar reactions carried out with cob(I)inamide were also second-order (Figure I, Supporting Information). The rate constant difference between the cobalamin and cobinamide systems in this model reaction is small (1.2-fold for  $PhNMe_3^+Cl^-$ , 2.4-fold for  $PhNMe_3^+I^-$ ), in good agreement with the small differences observed for reaction of cob(I)alamin and cob(I)inamide with  $CH_3-H_4$ folate bound to MetH(2–649).

## DISCUSSION

**Calculation of the Free Energy Profiles for the  $CH_3-H_4$ folate:Cob(I)alamin and  $CH_3-H_4$ folate:Cob(I)inamide Methyltransferase Reactions.** The  $\Delta G^\ddagger$  values for the forward and reverse methyl transfer reactions involving cobalamin and cobinamide can be derived from the rate constants listed in Table 1 using eq 1

$$\Delta G^\ddagger = -RT \ln \left( \frac{k_{cat}}{K_m} \right) \frac{h}{k_B T} \quad (1)$$

from transition-state theory (25, 26). In this equation,  $h$  is

Table 1: Second-Order Rate Constants for Methyl Transfers between Folate and Cobalamin/Cobinamide Catalyzed by MetH(2–649)

reaction	$k_{\text{cat}}/K_m$ (cofactor) ( $\text{M}^{-1} \text{s}^{-1}$ )	source	reaction	$k_{\text{cat}}/K_m$ (cofactor) ( $\text{M}^{-1} \text{s}^{-1}$ )	source
$\text{Co(I)Cbl}^- + \text{CH}_3\text{-H}_4\text{folate}$	$590 \pm 60^a$	8	$\text{MeCbl} + \text{H}_4\text{folate}$	$80 \pm 13$	24
$\text{Co(I)Cbl}^- + \text{CH}_3\text{-H}_4\text{folate}$	$620 \pm 40^b$	this work	$\text{MeCbl} + \text{H}_4\text{folate}$	$81 \pm 10^d$	this work
$\text{Co(I)Cbi} + \text{CH}_3\text{-H}_4\text{folate}$	$230 \pm 10^c$	this work	$\text{MeCbi}^+ + \text{H}_4\text{folate}$	$2800 \pm 400^e$	this work

<sup>a</sup> Standard errors were determined by averaging repetitive experiments. <sup>b</sup> Measured at 37 °C with the following initial concentrations of reagents:  $\text{CH}_3\text{-H}_4\text{folate}$ , 1 mM;  $\text{MetH(2-649)}$ , 6  $\mu\text{M}$ ; hydroxocobalamin, 100  $\mu\text{M}$ .  $\text{Cob(I)alamin}$  was generated by reduction with titanium citrate prior to initiation of the reaction. Results from five experiments were averaged to obtain the standard error. <sup>c</sup> Measured at 37 °C with the following initial concentrations of reagents:  $\text{CH}_3\text{-H}_4\text{folate}$ , 1 mM;  $\text{MetH(2-649)}$ , 6  $\mu\text{M}$ ; methylcobinamide, 65  $\mu\text{M}$ .  $\text{Cob(I)inamide}$  was generated by photolysis of methylcobinamide followed by reduction of the resultant  $\text{cob(II)inamide}$  to  $\text{cob(I)inamide}$  with titanium citrate. Results from five experiments were averaged to obtain the standard error. <sup>d</sup> Measured at 37 °C with the following initial concentrations of reagents:  $\text{H}_4\text{folate}$ , 4 mM;  $\text{MetH(2-649)}$  9.6  $\mu\text{M}$ ; methylcobalamin, 330  $\mu\text{M}$ . Results from five experiments were averaged to obtain the standard error. <sup>e</sup> Measured at 37 °C with the following initial concentrations of reagents:  $\text{H}_4\text{folate}$ , 4 mM;  $\text{MetH(2-649)}$ , 12.5  $\mu\text{M}$ ; methylcobinamide, 125  $\mu\text{M}$ . Results from four experiments were averaged to obtain the standard error.

Table 2: Comparisons of the Reactivity of Cobalamin and Cobinamide in Model Reactions

reaction	$k$ ( $\text{M}^{-1} \text{s}^{-1}$ )	source	reaction	$k$ ( $\text{M}^{-1} \text{s}^{-1}$ )	source
$\text{Co(I)Cbl}^- + \text{PhNMe}_3^+\text{Cl}^-$	$1.3 \times 10^{-3}$	this work	$\text{Co(I)Cbi} + \text{PhNMe}_3^+\text{I}^-$	$1.0 \times 10^{-3}$	this work
	$2 \times 10^{-3}$	17 <sup>a</sup>	$\text{MeCbl} + \text{RS}^- (\text{Hcy})$	$<0.1 \times 10^{-3}$	5 <sup>b</sup>
$\text{Co(I)Cbl}^- + \text{PhNMe}_3^+\text{I}^-$	$2.4 \times 10^{-3}$	this work	$\text{MeCbi}^+ + \text{RS}^- (\text{Hcy})$	$1.5 \times 10^{-3}$	5 <sup>b</sup>
$\text{Co(I)Cbi} + \text{PhNMe}_3^+\text{Cl}^-$	$1.0 \times 10^{-3}$	this work			

<sup>a</sup> The buffer was not specified. The rate of reaction was said to be independent of pH between 4 and 10. <sup>b</sup> Reactions were conducted under anaerobic conditions at pH 12 in the presence of 1 mM EDTA and  $\text{NaBH}_4$ .

Table 3: Forward and Reverse  $\Delta G$  and  $\Delta G^\ddagger$  Values Calculated from the Observed Rate Constants at 37 °C

reaction coordinate	kinetic value (kcal/mol)	reaction coordinate	kinetic value (kcal/mol)	reaction coordinate	kinetic value (kcal/mol)
$\Delta G_f^\ddagger(\text{Cbl})$	$14.2 \pm 0.1^a$	$\Delta G_r^\ddagger(\text{Cbi})$	$14.8 \pm 0.1$	$\Delta \Delta G_{\text{rxn}}$	$2.8 \pm 0.2$
$\Delta G_r^\ddagger(\text{Cbl})$	$15.5 \pm 0.1$	$\Delta G_f^\ddagger(\text{Cbi})$	$13.3 \pm 0.2$	$\Delta \Delta G_f^\ddagger$	$0.6 \pm 0.1$
$\Delta G_{\text{rxn}}(\text{Cbl})$	$-1.3 \pm 0.1$	$\Delta G_{\text{rxn}}(\text{Cbi})$	$1.5 \pm 0.2$	$\Delta \Delta G_r^\ddagger$	$-2.2 \pm 0.2$

<sup>a</sup> While the error bars reported in the Supporting Information were derived from least-squares analysis of the initial rates of *individual* reactions, the variations in values associated with repetitive determinations of the rate constants are greater (see Table I). Here we report  $2\sigma$  standard errors derived from repetitive experiments.

Planck's constant and  $k_B$  is Boltzman's constant. These values are shown in Table 3. From the values obtained in the forward and reverse directions of a reaction, the  $\Delta G_{\text{rxn}}(\text{Cbl})$  and  $\Delta G_{\text{rxn}}(\text{Cbi})$  can be calculated using eq 2. Using eqs 3 and 4,

$$\Delta G_{\text{rxn}} = \Delta G_f^\ddagger - \Delta G_r^\ddagger \quad (2)$$

$$\Delta \Delta G_f^\ddagger = \Delta G_f^\ddagger(\text{Cbi}) - \Delta G_f^\ddagger(\text{Cbl}) \quad (3)$$

$$\Delta \Delta G_r^\ddagger = \Delta G_r^\ddagger(\text{Cbi}) - \Delta G_r^\ddagger(\text{Cbl}) \quad (4)$$

we can calculate  $\Delta \Delta G_f^\ddagger$  and  $\Delta \Delta G_r^\ddagger$ . The free energy profiles derived from these values are shown in Figure 9. The value of  $0.6 \pm 0.1$  kcal/mol for  $\Delta \Delta G_f^\ddagger$  corresponds to the *acceleration* of methyl transfer from  $\text{CH}_3\text{-H}_4\text{folate}$  to  $\text{cob(I)alamin}$  due to the presence of dimethylbenzimidazole rather than the weaker water axial base. The positive value indicates that reaction of  $\text{cob(I)alamin}$  is characterized by a smaller activation energy than that of  $\text{cob(I)inamide}$ . In the ground state of the forward reaction, neither the intramolecular base dimethylbenzimidazole nor the exogenous base water is expected to be coordinated to the cobalt due to the  $\text{Co-N(bzm)}$   $\sigma$ -antibonding interaction associated with occupancy of the  $d_{z^2}$  orbital,<sup>2</sup> so the effect of the base is

presumably due to the formation of a stabilizing partial  $\text{Co-N(bzm)}$  bond in the transition state for the reaction.

The value of  $-2.2 \pm 0.2$  kcal/mol for  $\Delta \Delta G_r^\ddagger$  corresponds to the *deceleration* of methyl transfer from methylcobalamin to  $\text{H}_4\text{folate}$  due to the presence of the  $\text{Co-N(bzm)}$  bond from the intramolecular axial base dimethylbenzimidazole in methylcobalamin. The negative value indicates that methylcobalamin encounters a 2.2 kcal/mol higher energy barrier than methylcobinamide. This difference is consistent with decreased strength of the  $\text{Co-N(bzm)}$  bond in the transition state for the reaction as compared to the methylcobalamin ground state and with the stabilization of the ground-state methylcobalamin by bonding to dimethylbenzimidazole.

As expected for a reaction in which the product methylcobalamin is stabilized by axial ligation, but the reactant  $\text{cob(I)alamin}$  is not,  $\Delta G_{\text{rxn}}(\text{Cbl})$  is estimated to be  $-1.3$  kcal/mol, while  $\Delta G_{\text{rxn}}(\text{Cbi})$  is  $+1.5$  kcal/mol. The value of 2.8 cal/mol for the differential free energy  $\Delta \Delta G_{\text{rxn}}$  can be compared with the value of 3.3 kcal/mol determined independently by Kräutler from measurements of the equilibrium constant for methyl transfer between methylcobinamide and  $\text{cob(I)alamin}$  shown in eq 5 (27).

$$K_{\text{eq}} = \frac{[\text{cob(I)alamin}][\text{methylcobinamide}]}{[\text{methylcobalamin}][\text{cob(I)inamide}]} \quad (5)$$

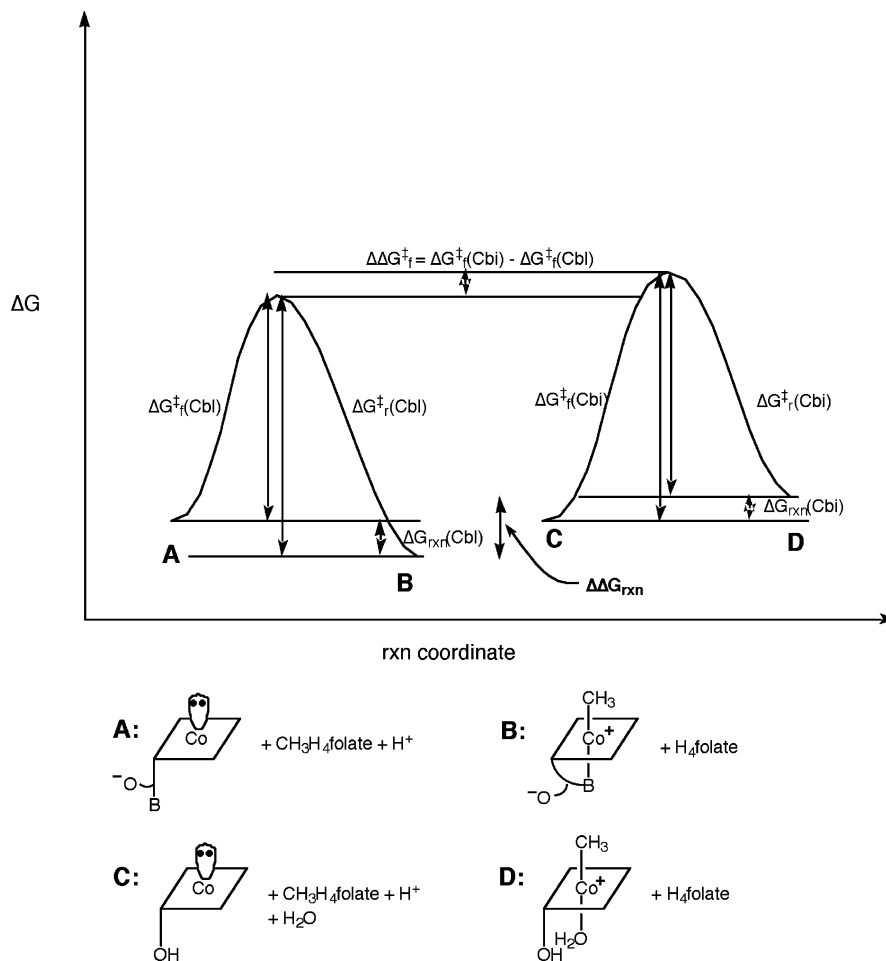


FIGURE 9: Calculated free energy profiles for methyl transfer between cob(I)alamin (left) or cob(I)inamide (right) and CH<sub>3</sub>-H<sub>4</sub>folate. The calculations, and the kinetic parameters on which they are based, are described in detail in the text.

The measurements of Kräutler were quite precise;  $K_{eq}$  is reported to be  $0.004 \pm 0.003$  from equilibria reached starting with methylcobalamin and cob(I)inamide or methylcobinamide and cob(I)alamin. However, the limits on  $\Delta\Delta G_{rxn}$  would thus range from 2.9 to 4.1 kcal/mol. The equilibrations were performed in 20 mM phosphate buffer, pH 7, at room temperature, while our kinetic measurements have been performed in 50 mM potassium phosphate buffer, pH 7.2, at 37 °C. Given these differences, we think the agreement between our values and Kräutler's is quite good. Our work allows the insight that the forward reaction provides 0.6 kcal/mol or 21% of the energetic difference, while the reverse reaction provides 2.2 kcal/mol or 79% of the energetic difference.

**Mechanistic Implications of the Reaction Profiles.** The salient finding of this study is that the strength of ligation of the axial base has only a *small effect* on the rates of group transfer from methyltetrahydrofolate to cob(I)alamin or cob(I)inamide. These findings have the important implication that the replacement of dimethylbenzimidazole by imidazole associated with binding of methylcobalamin to full-length MetH is not primarily a strategy for accelerating the rate of methyl transfer between the cofactor and the folate substrate. Instead, this axial base replacement has other roles, primarily in controlling the distribution of enzyme conformations during catalytic turnover (28).

When the ligand replacement associated with binding of methylcobalamin to MetH was first reported (29), our

laboratory and many others speculated that the histidine ligand might modulate the stability and reactivity of cobalamin in methionine synthase. The observation that the His759 ligand is connected by a hydrogen bond network to conserved residues Asp757 and Ser810 (29), and that this "ligand triad" is protonated when the enzyme is in the cob(I)alamin form (6), suggested involvement of the ligand triad in facilitating the change between base-off cob(I)alamin and base-on methylcobalamin during catalytic turnover. Indeed, replacement of the histidine ligand by glycine in MetH leads to abolition of catalytic activity (30). Since that time, a growing body of indirect evidence against a major role in catalysis for ligand replacement has been accumulating. Resonance Raman measurements showed that the Co—C stretching frequencies of methylcobalamin were unaffected by the *trans* ligand substitution induced by protonation of the dimethylbenzimidazole ligand (31). More recently, computational analysis of the spectra of alkylcobalamins using density functional theory has shown that removal of the dimethylbenzimidazole base from methylcobalamin to generate methylcobinamide hardly alters the Co—methyl bond at least in the ground state (2). Mounting evidence accumulated to suggest that the primary effect of removal of the histidine ligand is on the distribution of conformers of methionine synthase; the His759Gly mutant protein exists largely as a conformer in which the B<sub>12</sub> has access to adenosylmethionine but not to Hcy and CH<sub>3</sub>-H<sub>4</sub>folate and is therefore inactive because it does not contact its substrates (28, 30, 32).



The present studies provide direct evidence that the rates of methyl transfer between exogenous cobalamin cofactor and folate substrate bound to MetH(2–649) are little influenced by the strength of axial ligation to the cobalt. The results are consistent with an  $S_N2$  mechanism for methyl transfer from  $\text{CH}_3\text{-H}_4\text{folate}$  to cob(I)alamin, but one in which coordination of the dimethylbenzimidazole nitrogen to cobalt lags behind formation of the carbon–cobalt bond. Our studies suggest that the Co–N bond is relatively weak in the transition state as compared to the methylcobalamin ground state, thus accounting for the relatively small effect of axial ligation on the reaction rate in the reverse direction.

One published study compares the rates of reaction of methylcobalamin and methylcobinamide with alkanethiolates (5), and the rate constants obtained are provided in Table 2. The measurements were conducted at pH 12 in the presence of EDTA and  $\text{NaBH}_4$ . Under these conditions methylcobalamin reacted with homocysteinethiolate at least 1500-fold more slowly than methylcobinamide, a much larger deceleration than we have observed. The large difference in rate constants observed in this model reaction suggests that all bonding to the dimethylbenzimidazole nitrogen must be lost in the transition state. This observation contrasts with the MetH-catalyzed transition state, with its apparent partial bonding to dimethylbenzimidazole and much smaller differences (35-fold) in the rates of reaction of methylcobalamin and methylcobinamide.

Many corrinoid-dependent enzymes retain the ability to react with exogenous cobalamin as well as with their physiological substrates, which are proteins containing bound corrinoids.<sup>3</sup> In regimes where these reactions are first-order in the corrinoid cofactor, the second-order rate constants for the reactions can be compared with the second-order rate constants for the corresponding chemical model reactions. The one published study in which second-order rate constants for reactions involving methylcobalamin and methylcobinamide have been compared is of acetyl-CoA synthase (4). Acetyl-CoA synthase utilizes a methylated corrinoid/iron–sulfur protein as a methyl donor to an enzyme-bound metallocofactor in the synthesis of acetyl-CoA; the corrinoid cofactor is 5-methoxybenzimidazolylcobamide. Acetyl-CoA synthase can also use exogenous methylcobalamin or methylcobinamide as a substitute for the methylated corrinoid iron–sulfur protein. The rate constant for methyl transfer from exogenous methylcobinamide of  $200 \text{ M}^{-1} \text{ s}^{-1}$  is more than 2000-fold faster than that for methyl transfer from methylcobalamin of  $<0.12 \text{ M}^{-1} \text{ s}^{-1}$ , a much greater difference than the 35-fold difference that we found for MetH in this study, but comparable to the rate constant differences seen in the model reactions.<sup>4</sup>

The methylated corrinoid iron–sulfur protein which is the physiological methyl donor for acetyl-CoA synthase shows the spectral properties of a “base-off corrinoid”, indicating that the nucleotide substituent is not coordinated to the cobalt of the corrin (33). In fact, the protein remains “base-off” in all cobalt oxidation states (34). Methyl transfer from exogenous methylcobalamin to acetyl-CoA synthase also appears

not to involve any stabilization of the transition state by bonding of an axial base. In contrast, the intrinsic methylcobalamin cofactor of full-length MetH is base-on as is the cob(II)alamin form of the bound cofactor, so the observation of partial bonding of the dimethylbenzimidazole of the exogenous cofactor in the transition state for the  $\text{CH}_3\text{-H}_4\text{folate:cob(I)alamin}$  methyltransferase reaction is not surprising.

When the rate constants for the enzyme-catalyzed reactions of exogenous cobalamin and cobinamide cofactors are compared with those of the model systems, the most striking feature is the large rate acceleration characteristic of the reactions with enzyme-bound substrates. Thus, the rate constant for reaction of exogenous cob(I)inamide with  $\text{CH}_3\text{-H}_4\text{folate}$  bound to MetH(2–649) is  $2800 \text{ M}^{-1} \text{ s}^{-1}$ , while the rate constant for reaction of cob(I)inamide with  $\text{PhNMe}_3^+\text{I}^-$  is  $2 \times 10^{-3} \text{ M}^{-1} \text{ s}^{-1}$ , slower by a factor of  $1.4 \times 10^6$ . Although the methyl donor substrates are very different ( $\text{CH}_3\text{-H}_4\text{folate}$  vs  $\text{PhNMe}_3^+$ ), the intriguing point here is that the kinetic advantage is to the nominally uncharged poorer methyl donor  $\text{CH}_3\text{-H}_4\text{folate}$  rather than to the intrinsically better cationic methyl donor  $\text{PhNMe}_3^+$ . The enhanced reactivity of enzyme-bound  $\text{CH}_3\text{-H}_4\text{folate}$  is consistent with kinetic evidence that protonation of  $\text{CH}_3\text{-H}_4\text{folate}$  occurs in the enzyme· $\text{CH}_3\text{-H}_4\text{folate}$ ·cob(I)alamin ternary complex (12). The increased rate of enzymatic methyl transfer also is likely to reflect desolvation of the polar reactants in the enzyme-catalyzed reaction, as in simple solution analogues (35).

The folate-binding module of MetH shows sequence similarity with the methyl transferase subunit AcsE of acetyl-CoA synthase, which is responsible for the methylation of the corrinoid/iron–sulfur subunit of acetyl-CoA synthase (36). The structure of AcsE has been determined;  $\text{CH}_3\text{-H}_4\text{folate}$  is bound in the inside of a  $\beta_8\alpha_8$  barrel (37). Binding of cob(I)alamin would be expected to cover the top of the barrel, shielding the reacting  $\beta$ -face of the cobalamin and the folate substrate from solvent.  $S_N2$  reactions involving a pair of polar reactants are greatly accelerated in media with low dielectric constants (35), and the environment of the transient complex formed between the  $\text{CH}_3\text{-H}_4\text{folate}$  bound to MetH(2–649) and cob(I)alamin would be expected to be characterized by a greatly reduced dielectric constant as compared to the aqueous solvated compounds in the model reactions.

**Conclusions.** The second-order rate constant for reaction of cob(I)alamin with  $\text{CH}_3\text{-H}_4\text{folate}$  bound to MetH(2–649) is 2.7-fold faster than that for reaction of cob(I)inamide; in the reverse direction, methylcobinamide reacts 35-fold faster with enzyme-bound  $\text{H}_4\text{folate}$  than methylcobalamin. These measurements allow a detailed analysis of the reaction profiles for both species, resulting in the conclusion that the

<sup>3</sup> Corrinoids are corrin cofactors that contain a variety of nucleotide substituents, and include cobalamins with the dimethylbenzimidazole nucleotide substituent as a special case. The nucleotide substituent may or may not coordinate to the cobalt atom.

<sup>4</sup> The measured values for  $\Delta\Delta G_{\text{rxn}}$  range from 2.8 to 4.0 kcal/mol, as discussed in the text. If there were no bonding to the base in the transition state for methyl transfer, we would expect that methylcobalamin would react  $\sim 100$ – $1000$ -fold more slowly than methylcobinamide. The 1500–2000-fold decreased rates of reaction of methylcobinamide as compared to methylcobalamin reported in the literature may reflect the presence of impurities in methylcobinamide (3) and/or differences in the reaction conditions employed for these experiments. In particular, experiments probing methyl transfer to CO dehydrogenase were performed at  $55^\circ\text{C}$  and pH 7.6 (4), while experiments probing the reactivity of methylcobamides with thiols were performed at pH 12 (5).

axial base provides a 0.6 kcal/mol stabilization in the forward reaction, 22% of the total possible stabilization, implying a partial Co–N(bzm) bond in the transition state. The magnitude of the effect of the axial base on the rate constant for the forward reaction is small ( $\sim 3$ -fold) compared to the overall activation of methyl transfer to cob(I)alamin ( $\sim 10^6$ -fold), implying that the appended histidine ligand in the holoenzyme is not primarily involved in accelerating an elementary step in the catalytic cycle. These results are consistent with the hypothesis that the ligand triad in methionine synthase is not primarily involved in accelerating the rate of methyl group transfer, but rather is important for controlling the distribution of enzyme conformations during catalysis.

## ACKNOWLEDGMENT

We thank Kenneth Doll for helpful comments on the manuscript.

## SUPPORTING INFORMATION AVAILABLE

Two figures demonstrating first-order dependence of  $\text{CH}_3\text{-H}_4\text{folate:cob(I)inamide}$  methyltransferase activity on the concentrations of cob(I)inamide and enzyme, two figures demonstrating first-order dependence of  $\text{H}_4\text{folate:methylcobinamide}$  methyltransferase activity on the concentrations of methylcobinamide and enzyme, three figures documenting the effect of pyridine on methyltransferase reactions, and two figures documenting the dependence of  $\text{PhNMe}_3^+\text{Cl}^-$ -cob(I)alamin/cob(I)inamide methyltransferase activity on  $\text{PhNMe}_3^+\text{Cl}^-$ . This material is available free of charge via the Internet at <http://pubs.acs.org>.

## REFERENCES

1. Lexa, D., and Saveant, J. M. (1976) *J. Am. Chem. Soc.* 98, 2652–2658.
2. Stich, T. A., Brooks, A. J., Buan, N. R., and Brunold, T. C. (2003) *J. Am. Chem. Soc.* 125, 5897–5914.
3. Sirovatka, J. M., Matthews, R. G., and Finke, R. G. (2002) *Inorg. Chem.* 41, 6217–6224.
4. Seravalli, J., Brown, K. L., and Ragsdale, S. W. (2001) *J. Am. Chem. Soc.* 123, 1786–1787.
5. Norris, P. R., and Pratt, J. M. (1996) *BioFactors* 5, 240–241.
6. Jarrett, J. T., Choi, C. Y., and Matthews, R. G. (1997) *Biochemistry* 36, 15739–15748.
7. Drummond, J. T., Huang, S., Blumenthal, R. M., and Matthews, R. G. (1993) *Biochemistry* 32, 9290–9295.
8. Goulding, C. W., Postigo, D., and Matthews, R. G. (1997) *Biochemistry* 36, 8082–8091.
9. Banerjee, R. V., Johnston, N. L., Sobeski, J. K., Datta, P., and Matthews, R. G. (1989) *J. Biol. Chem.* 264, 13888–13895.
10. Hall, D. A., Jordan-Starck, T. C., Loo, R. O., Ludwig, M. L., and Matthews, R. G. (2000) *Biochemistry* 39, 10711–10719.
11. Zydowsky, T. M., Courtney, L. F., Frasca, V., Kobayashi, K., Shimizu, H., Yuen, L.-D., Matthews, R. G., Benkovic, S. J., and Floss, H. G. (1986) *J. Am. Chem. Soc.* 108, 3152–3153.
12. Matthews, R. G., Smith, A. E., Zhou, Z. S., Taurog, R., Bandarian, V., Evans, J. C., and Ludwig, M. L. (2003) *Helv. Chim. Acta*, in press.
13. Evans, J. C., Huddler, D. P., Hilgers, M. T., Romanchuk, G., Matthews, R. G., and Ludwig, M. L. (2003) *Proc. Natl. Acad. Sci. U.S.A.*, in press.
14. Hilhorst, E., Iskander, A. S., Chen, T. B. R. A., and Pandit, U. K. (1994) *Tetrahedron* 50, 8863–8870.
15. Zheng, D., Darbre, T., and Keese, R. (1999) *J. Inorg. Biochem.* 77, 273–275.
16. Wedemeyer-Exl, C., Darbre, T., and Keese, R. (1999) *Helv. Chim. Acta* 82, 1173–1184.
17. Pratt, J. M., Norris, P. R., Hamza, M. S. A., and Bolton, R. (1994) *J. Chem. Soc., Chem. Commun.* 1994, 1333–1334.
18. Goulding, C. W., and Matthews, R. G. (1997) *Biochemistry* 36, 15749–15757.
19. Zehnder, A. J., and Wuhrmann, K. (1976) *Science* 194, 1165–1166.
20. Shriver, D. F., and Drezdon, M. A. (1986) *The manipulation of air-sensitive compounds*, John Wiley & Sons, New York.
21. Hill, J. A., Pratt, J. M., and Williams, R. J. P. (1964) *J. Chem. Soc.* 1964, 5149–5153.
22. Klibanov, A. M. (1997) *Trends Biotechnol.* 15, 97–101.
23. Cowan, D. A., and Plant, A. R. (1992) in *Biocatalysts at extreme temperatures* (Adams, M. W. W., and Kelly, R. M., Eds.) pp 86–107, American Chemical Society, Washington, DC.
24. Smith, A. E. (2001) Ph.D. Thesis, Department of Medicinal Chemistry, University of Michigan, 140 pp.
25. Frost, A. A., and Pearson, R. G. (1961) *Kinetics and mechanism*, 2nd ed., John Wiley and Sons, New York.
26. Fersht, A. (1985) *Enzyme structure and mechanism*, 2nd ed., W. H. Freeman and Co., New York.
27. Kräutler, B. (1987) *Helv. Chim. Acta* 70, 1268–1278.
28. Bandarian, V., Ludwig, M. L., and Matthews, R. G. (2003) *Proc. Natl. Acad. Sci. U.S.A.* 100, 8156–8163.
29. Drennan, C. L., Huang, S., Drummond, J. T., Matthews, R. G., and Ludwig, M. L. (1994) *Science* 266, 1669–1674.
30. Jarrett, J. T., Amaratunga, M., Drennan, C. L., Scholten, J. D., Sands, R. H., Ludwig, M. L., and Matthews, R. G. (1996) *Biochemistry* 35, 2464–2475.
31. Dong, S., Padmakumar, R., Banerjee, R. V., and Spiro, T. G. (1996) *J. Am. Chem. Soc.* 118, 9182–9183.
32. Bandarian, V., Patridge, K. A., Lennon, B. W., Huddler, D. P., Matthews, R. G., and Ludwig, M. L. (2002) *Nat. Struct. Biol.* 9, 53–56.
33. Ragsdale, S. W., Lindahl, P. A., and Münck, E. (1987) *J. Biol. Chem.* 262, 14289–14297.
34. Wirt, M. D., Kuman, M., Wu, J., Scheuring, E. M., Ragsdale, S. W., and Chance, M. R. (1995) *Biochemistry* 34, 5269–5273.
35. March, J. (1992) *Advanced organic chemistry*, 4th ed., John Wiley & Sons, New York.
36. Roberts, D. L., Zhao, S., Doukov, T., and Ragsdale, S. W. (1994) *J. Bacteriol.* 176, 6127–6130.
37. Doukov, T., Seravalli, J., Stezowski, J. J., and Ragsdale, S. W. (2000) *Structure* 8, 817–829.

BI035525T